

## Application of Bimetallic Nanoparticles as Eco-Friendly Metal Corrosion Inhibitors in a Thiol Medium Through the Example of Cysteine

Gulzhan Daumova<sup>1</sup>, Yelena Van<sup>2</sup>, Yakov Masyutin<sup>2</sup>,  
Anton Gradov<sup>2</sup>, Yelena Ivashchenko<sup>1\*</sup>

<sup>1</sup> D. Serikbayev East Kazakhstan Technical University, 19, Serikbayev str., 070000, Ust-Kamenogorsk, Kazakhstan

<sup>2</sup> Immanuel Kant Baltic Federal University, 14 A. Nevskogo ul., 236016 Kaliningrad, Russia

\* Corresponding author's e-mail: en\_ivashchenko2020@mail.ru

### ABSTRACT

This article raises the relevancy problems of bimetallic nanostructures using to inhibit corrosion processes specific to various sulfur-containing media, including the extraction and transportation of natural hydrocarbons, in oil and gas condensate equipment. The environmental aspect of the research is the possibility of using bimetallic nanostructures modified with cysteine as environmentally friendly agents that protect steel from corrosion, especially in a thiol medium. There are presented experimental data on the synthesis and study of bimetallic nanostructures based on copper and silver in a thiol medium based on cysteine aminoacid. The research field is conditioned by these days' tendency that advanced developments in many branches of science are directly associated to the application of nanomaterials. The high action efficiency of these materials is achieved due to their highly dispersed state, distinguishing them favorably from conventional macroobjects. The synthesis of Cu/Ag nanostructures was carried out due to the unique properties of bimetals, such as increased activity of atoms in the surface layer, display of quantum effects, etc., that are more pronounced than those in monometallic nanostructures. The main article concept lies within simulation the process of sulfides and other sulfur compounds formation with bimetallic nanoparticles to protect oil and gas equipment from sulfur-containing corrosive agents in aqueous medium. The goal is to synthesize the copper-silver bimetallic microparticles stabilized with apple pectin and verification of the possibility of forming a metal-sulfur bond at the nanoscale level with cysteine aminoacid as a suitable and convenient compound. The objectives include directly the method of synthesis of the bimetallic microstructure Cu-Ag, stabilized with a solution of apple pectin; absorption spectrophotometry of the studied disperse system of bimetallic Cu-Ag microparticles in the visible region; scanning electron microscopy (SEM) of the bimetallic Cu-Ag microparticles obtained; study of chemisorption of L-cysteine hydrochloride on the dispersed phase surface of bimetallic Cu-Ag microparticles; Raman-scattering spectroscopy of the sample obtained after chemisorption.

**Keywords:** bimetallic microstructures Cu-Ag, eco-friendly agents, thiols, cysteine, corrosion.

### INTRODUCTION

Nowadays, oil is one of the main sources of hydrocarbons. The chemical composition of oil is quite diverse. It includes the following classes of substances as alkanes, cycloalkanes, arenes, as well as various oxygen-, nitrogen-, and sulfur-containing substances, resinous-asphaltenic substances, and many more [Yang et al., 2018]. In addition to organic substances, there are also mineral ones in oil composition. They include some water, as well as metal salts (V, Cr, Ni, Fe, Co, Mg, etc.)

in dissolved forms. In the article [Aleksandrova et al., 2017] the extraction of the following metals as vanadium, iron, cobalt, etc. from heavy oil of the Yaregskoye field in the Komi Republic, Russian Federation is investigated. The scientific group studied the dependence of the metals yields on the type of extracting solvent, its concentration and the conditions for metals concentrating. The optimal conditions for the extraction of these metals are kerosene or ethanol as extraction agents, while additional ultrasonic treatment enhances the process of metals concentrating in the organic phase.

The most valuable components of oil are its hydrocarbons. They are regularly used in the production of pharmaceuticals, detergents, in the transport industry as fuels for cars, trucks, etc., for the creation of car tires, roadway surfacing with high-boiling fractions, and in many other branches of industry and technology. In addition to hydrocarbons, oil contains various heteroatomic compounds. For instance, oil contains certain classes of sulfur-containing substances. These include thiols (RSH), hydrogen sulfide ( $H_2S$ ), thioethers (RSR'), sulfides ( $S^{2-}$ ), disulfides (RSSR'), thiophane derivatives, thiophene derivatives, and other classes and derivatives (Figure 1).

Oil transportation. The transportation and recovery of oil from the depths proceed under high pressures and temperatures, extremely exceeding normal conditions (273.14 K, 1 atm.). Some heteroatomic sulfur compounds are reactive enough to react with the oil pipeline hull. These ones include elemental sulfur, thiols and thioethers [Coutinho et al., 2022]. The rest are relatively inert and do not react with the hull. The main corrosion mechanism of such equipment is the formation of metal sulfides and a decrease in the impermeability and strength of the pipeline. Copper reacts very easily with sulfur-containing compounds to form copper sulfides  $Cu_2S$  and  $CuS$ , as well as aluminum and other metals. In oxygen-free systems, the reaction proceeds only to the formation of an insoluble sulfide deposit, while the presence of oxygen leads to further oxidation of sulfides to sulfites and sulfates:  $CuSO_4$ ,  $Al_2(SO_4)_3$  [Lewand, 2002]. Therefore, the pipelines protection from ecologically unfriendly sulfur-containing substances is an urgent problem.

Nowadays, advanced developments in many branches of science are directly associated to the nanomaterials using. Due to their highly dispersed state, they differ from conventional macroobjects

in their unique properties: bactericidal activity, increased thermal and electrical conductivity, etc. Such features can be explained by the high activity of the surface layer atoms and display the quantum effects in the structure of the material [Campos et al., 2019]. The practical application of nanoparticles and nanomaterials helps to solve many problems in various fields of science: ecology [Mamyachenkov et al., 2017], analytical chemistry, medicine [Peng and Lian, 2019], materials science, energetics, etc.

As of today, more and more attention is being paid to the creation of new bimetallic nanomaterials consisting of two types of metals, for example, Au/Pd, Au/Ag, Au/Pt [Zhong et al., 2020]. They exhibit the properties mentioned above better than monometallic ones. In recent years several research groups from different countries have made reports on the using of copper-silver nanoparticles as catalysts for transformations of such organic compounds as 4-nitrophenol [Wu et al., 2015], formaldehyde [Feng et al., 2018], etc.

The main idea of the present article is to simulate the formation of sulfides and other sulfur compounds with metal nanoparticles to protect oil and gas equipment from sulfur-containing corrosive agents in the aqueous medium. The experiments are planned to transfer in real conditions with the application of a nanoparticles layer on the surface of the pipeline hull and reproduce the near conditions for the transportation of oil through the pipe.

## MATERIALS AND METHODS

The goal of the article is to synthesize copper-silver bimetallic microparticles stabilized with apple pectin solution and testing the possibility of forming a metal-sulfur bond at the nanoscale

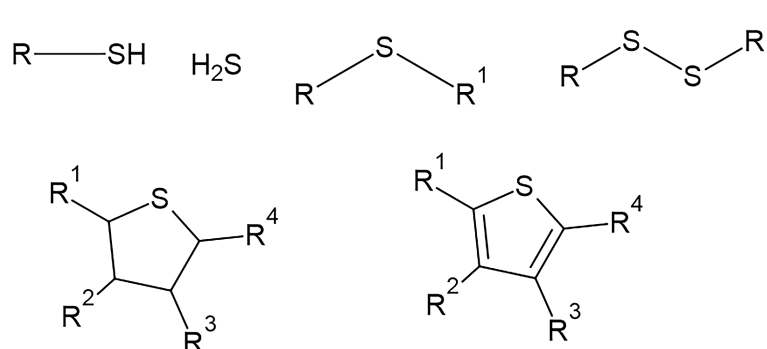
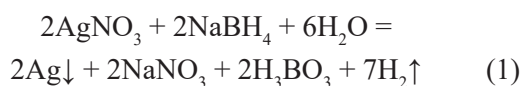


**Figure 1.** Examples of sulfur-containing substances that are part of oil [Coutinho et al., 2022]

level with easy-to-use cysteine aminoacid. The objectives of the study include directly the method of synthesis of the bimetallic microstructure Cu-Ag stabilized with a solution of apple pectin; absorption spectrophotometry of the studied disperse system in the visible region; scanning electron microscopy (SEM) of the bimetallic microparticles obtained; study of chemisorption of L-cysteine hydrochloride on the surface of the dispersed phase; Raman-scattering spectroscopy of the sample.

### Synthesis of Cu-Ag bimetallic microstructure stabilized with an apple pectin solution

To obtain stable bimetallic nanostructures, the most successful, simple, and highly efficient synthesis method turned out to be the reduction of cupric ions  $\text{Cu}^{2+}$  to metallic copper  $\text{Cu}^0$  on the surface of silver nanoparticles. The method consisted in obtaining a highly dispersed sol of silver nanoparticles with further deposition of copper particles on its surface, and stabilizing the resulting disperse system with a solution of apple pectin. To obtain silver nanoparticles, a chemical method was chosen by reducing silver ions  $\text{Ag}^+$ , using an aqueous solution of sodium tetrahydroborate in accordance with Equation 1:



In a 50 ml conical flask there was added 30.0 ml 0.002 mol/L  $\text{NaBH}_4$  solution and 2.00 ml 0.001 mol/L  $\text{AgNO}_3$  solution. Silver nitrate was added dropwise at a rate of 1 drop/sec. with vigorous stirring on a magnetic stirrer. After adding the required amount of silver nitrate solution, the stirring was stopped and a flask was placed on the stove to heat for 2 minutes at 80 °C [Wan et al., 2020]. During the reduction reaction, the color of the solution changed from colorless to yellow.

The deposition of copper on the surface of silver nanoparticles was carried out by the reduction of cupric ions on the surface of the initial dispersed phase. For that particular purpose, there was taken 5.00 ml of freshly prepared sol of silver nanoparticles into a 50 ml heat-resistant beaker, then 1.30 ml 0,007 mol/L  $\text{NaBH}_4$  was added as a reducing agent along with adding of 1.60 ml 0.0003 mol/L of  $\text{CuSO}_4$  aqueous solution and 4 ml of an apple pectin solution. A solution of apple pectin was prepared as follows: a 0.1 g sample was weighed on an analytical balance, dissolved

in 100 ml of water at 50 °C, heated and vigorously stirred for 15 minutes. After adding all the reagents, the sol was intensively stirred on a magnetic stirrer for 15 seconds to evenly distribute the substances throughout the entire volume of the dispersed system. After that the sol was heated for 3 minutes at 80 °C until the intensity of color changed [Wan et al., 2020].

### Absorption spectrophotometry of the studied disperse system of bimetallic Cu-Ag microparticles in the visible region

The absorption spectrum of disperse systems was obtained in the wavelength range from 350 to 800 nm with a two-beam scanning spectrophotometer UV-1800 Shimadzu in a quartz optical cell with a 1 cm optical path length. Distilled water was used as a reference solution. Baseline correction was always performed prior to collecting the spectral data on the studied disperse system to equate the background signals to zero over the entire selected wavelength range.

### Scanning electron microscopy (SEM) of bimetallic Cu-Ag microparticles

A silica support with dimensions of 1x1 cm was immersed in a mixture of acetone and ethanol in a ratio of 1:1 for 15 minutes in an ultrasonic chamber. Then the support was transferred to a special chamber for cleaning under low vacuum with gas-discharge plasma for 10 minutes. Then there was applied 1 drop of the dispersed system with a pipette to the cleaned  $\text{SiO}_2$  surface, and sent to a chamber under low vacuum to remove water for 15 minutes. The prepared sample was loaded into a scanning electron microscope and images of the dispersed system were obtained.

### Study of the chemisorption of L-cysteine hydrochloride on the surface of the dispersed phase of bimetallic Cu-Ag microparticles

In a 50 ml measuring cup there were placed 11.90 ml sol of bimetallic Cu-Ag microparticles, stabilized with a solution of apple pectin, and 2.40 ml L-cysteine hydrochloride with a number of concentrations:  $10^{-3}$ ,  $10^{-4}$ ,  $10^{-5}$ , and  $10^{-6}$  mol/L. The pH value was varied in the range of 6.0–10.5, using a 0.1 mol/L ammonia solution  $\text{NH}_3 \cdot \text{H}_2\text{O}$  and an acetate buffer solution with pH = 5. The acidity of medium was monitored using a pH-meter.

The resulting solution was left in a thermostat at a temperature of 25 °C for 24 hours.

### Raman-scattering spectroscopy of the sample obtained after chemisorption

The samples after chemisorption were evaporated to a volume of 5 ml prior to the Raman spectroscopy, and a sample drop was placed on a silicon support with a layer of 200 nm thick vanadium deposit. Then the drop was dried at 35 °C, and the spectrum was collected with a Horiba Jobin Yvon LabRam HR800 Raman spectrometer at the edge of the dried drop. A He-Ne laser with a wavelength of 632.8 nm was used for excitation. The power of laser radiation on the sample was 0.5 mW, and the beam size was about  $10 \times 10 \mu\text{m}$ . The spectrum was taken in the range of  $100\text{--}1900 \text{ cm}^{-1}$  and  $2400\text{--}3000 \text{ cm}^{-1}$ .

## RESULTS

### Characteristics of the sol of bimetallic Cu-Ag microparticles

As known, metal sols are capable of absorbing light in the visible region of the spectrum. To confirm the successful synthesis of a disperse system, an absorption spectrum was recorded. The

spectrum had a flat peak with an absorbance of 0.50 at a wavelength of 415 nm (Figure 2). The microphotographs of a sol of bimetallic copper-silver particles stabilized with apple pectin were obtained, using SEM method (Figure 3).

### Study of L-cysteine hydrochloride chemisorption on the surface of bimetallic Cu-Ag microparticles

A thiol group in the cysteine molecule makes it possible to use it as a modeling corrosive agent. Therefore, cysteine was chosen to check the possibility of metal-sulfur bond formation. Chemisorption of L-cysteine hydrochloride depends on pH values (factor A) and adsorbate concentration (factor B). For example, pH values affect the processes of protonation, deprotonation, and as a result, the ratio of ionic forms of L-cysteine. In a strongly acidic medium, the protonation of the amino group occurs. In a slightly acidic medium, the amino group is also protonated, while the carboxyl group is deprotonated. In a slightly alkaline medium, the amino group is protonated, the carboxyl group is deprotonated, and the mercapto group is deprotonated. In a strongly alkaline medium, the deprotonation of the mercapto group and the carboxyl group occurs (Figure 4) [Wan et al., 2021]. The results of a spectrophotometric study of the chemisorption of L-cysteine

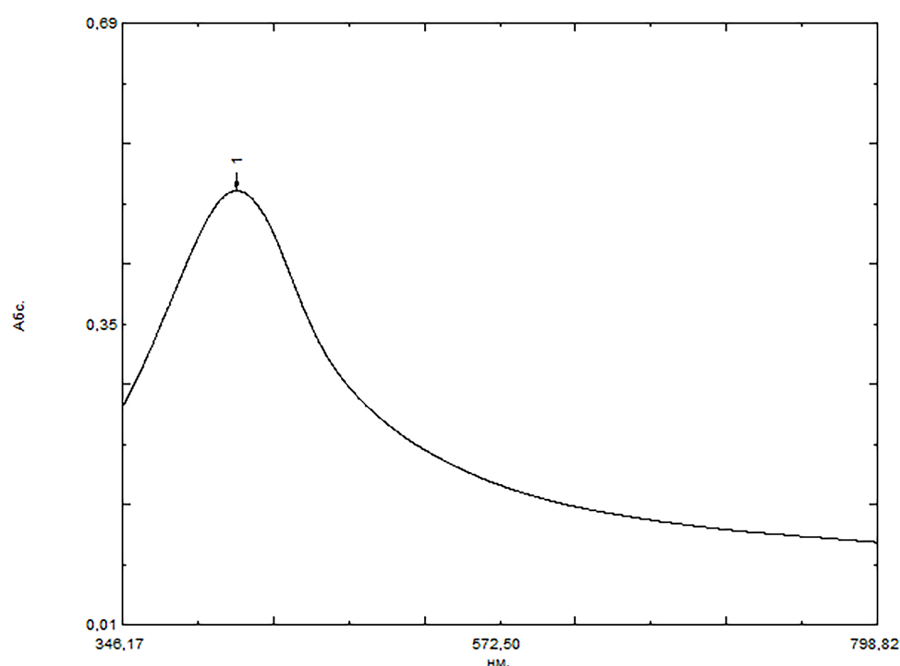


**Figure 2.** Absorption spectrum of a sol of bimetallic Cu-Ag microparticles stabilized with a solution of apple pectin



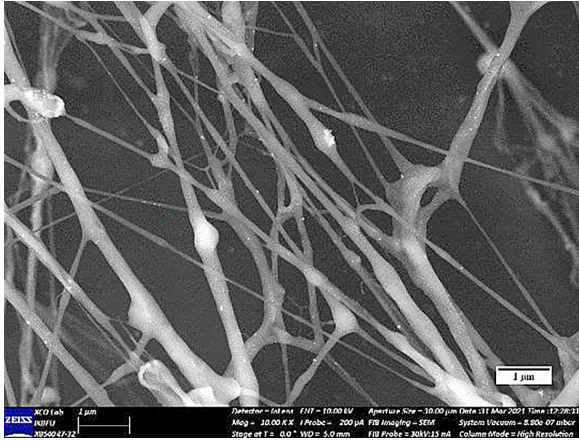


**Figure 3.** Micrograph of bimetallic Cu-Ag microparticles stabilized with apple pectin solution

hydrochloride are shown in Figure 5. In the case when the concentration of L-cysteine hydrochloride was  $10^{-3}$  mol/L (blue curve), the aggregation of the dispersed system occurred at high pH values, and the surface plasmon resonance (SPR) peak disappeared. This causes the interaction of charged ionic forms of L-cysteine with a double-electric layer of the dispersed phase particles.

At these relatively low concentrations of L-cysteine hydrochloride as  $10^{-4}$  (red curve),  $10^{-5}$  (yellow curve) and  $10^{-6}$  (green curve) mol/L, there was a slight change in the absorbance values, while with a decrease in pH values the absorbance gradually increased. In this case, the maximum values of light absorption fell on the pH

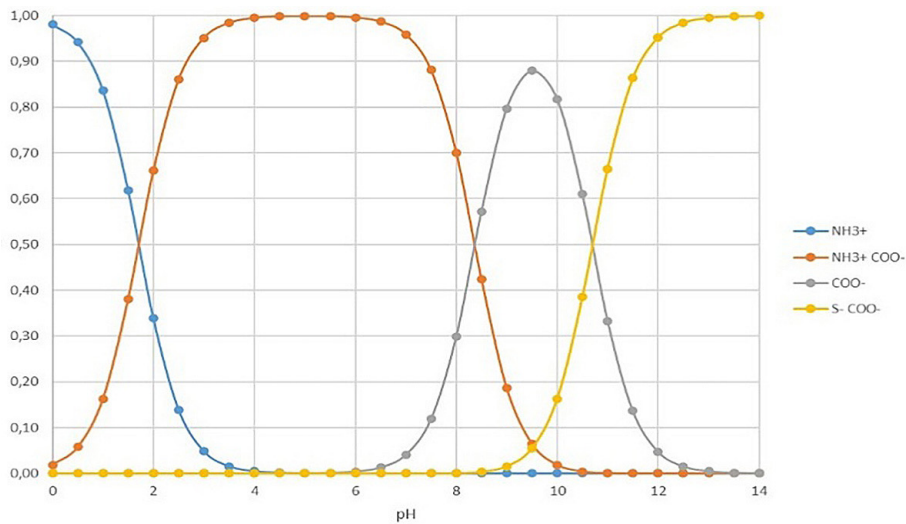


**Figure 4.** The distribution of ionic forms of L-cysteine depending on the pH values of the solution

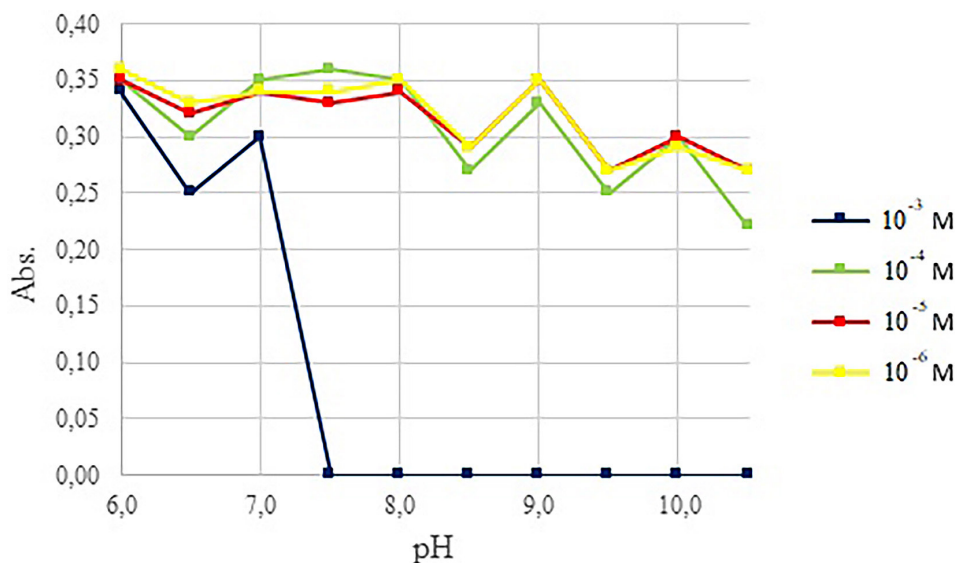


**Figure 5.** The dependence of the absorbance ( $\lambda_{\max} = 416\text{--}424$  nm) of the solution on pH 1 day after thermostatic control

range from 6 to 8. When moving towards a neutral and slightly acidic pH values, the mole fraction of the second (neutral) ionic form increases. To determine if there is a relationship between the absorbance value at each concentration of L-cysteine hydrochloride and the mole fraction of the neutral ionic form of L-cysteine hydrochloride (II form), the Pearson correlation coefficient was determined (Table 2 in the discussion section).

To prove the chemisorption process, the synthesized samples were studied using Raman spectroscopy. Since the maximum values of light absorption were in the pH range from 6 to 8, the study of the process was carried out only in this range. At  $10^{-3}$  mol/L concentration of L-cysteine hydrochloride, the following peaks were present in the Raman spectrum at each pH value: an S-S bond peak ( $500\text{ cm}^{-1}$ ), an Ag-S bond peak ( $240\text{ cm}^{-1}$ ), a characteristic pectin peak ( $850\text{ cm}^{-1}$ ) and the C-H bond peak ( $2900\text{ cm}^{-1}$ ), while the peak of the S-H bond ( $2574\text{ cm}^{-1}$ ) disappeared according to Figure 6.

Chemisorption occurred at this concentration of the adsorbate, but the formation of cystine (dimer of L-cysteine) also occurred due to the excess

of L-cysteine hydrochloride. In the case of a L-cysteine hydrochloride concentration of  $10^{-4}$  mol/L, a peak of the Ag-S bond appeared in the Raman spectrum of the same intensity as at  $10^{-3}$  mol/L adsorbate concentration. At the same time, the peak of the S-S ( $500\text{ cm}^{-1}$ ) and S-H ( $2574\text{ cm}^{-1}$ ) bonds did not appear, and the peaks of pectin ( $850\text{ cm}^{-1}$ ), the Ag-S ( $240\text{ cm}^{-1}$ ) and C-H ( $2900\text{ cm}^{-1}$ ) bonds appeared in accordance with Figure 7.

When the concentration of L-cysteine hydrochloride was  $10^{-5}$  and  $10^{-6}$  mol/L, the intensity of the Ag-S bond peak ( $240\text{ cm}^{-1}$ ) was very small, and all other peaks were of low intensity or were presented as blank noise. Thus, the process of chemisorption of L-cysteine hydrochloride proceeds most effectively at a pH value of 7.0 and an adsorbate concentration of  $10^{-4}$  mol/L in accordance with Figure 7.

## DISCUSSION

The particle size distribution was determined (Fig. 8) after the synthesis of a Cu-Ag bimetallic

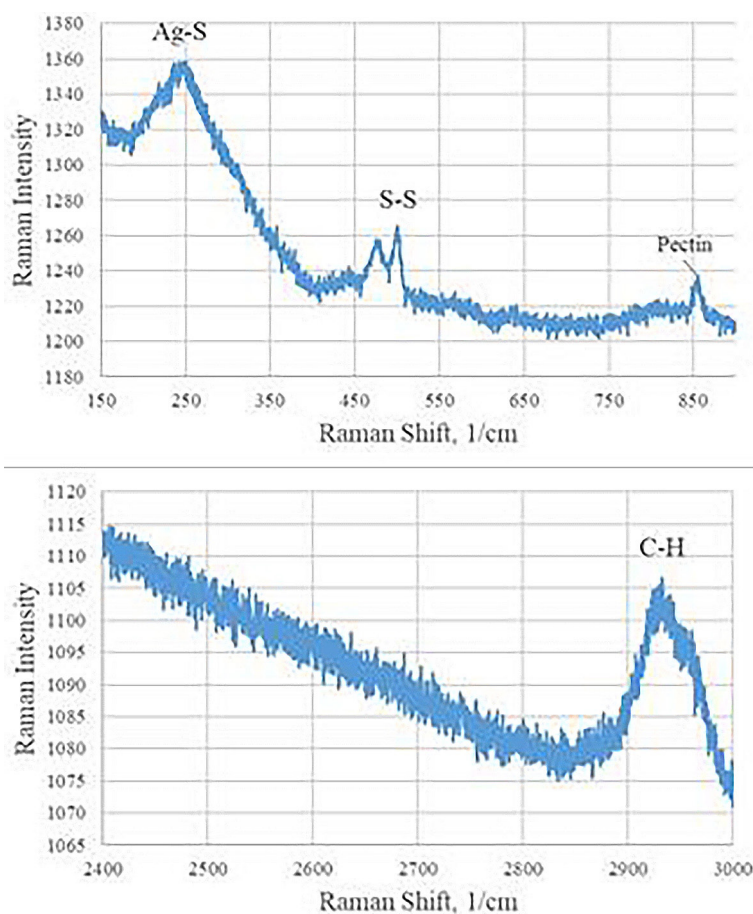


**Figure 6.** Raman-scattering spectrum of the sample (pH = 7.0,  $C(\text{cys-H}) = 10^{-3}$  mol/L)

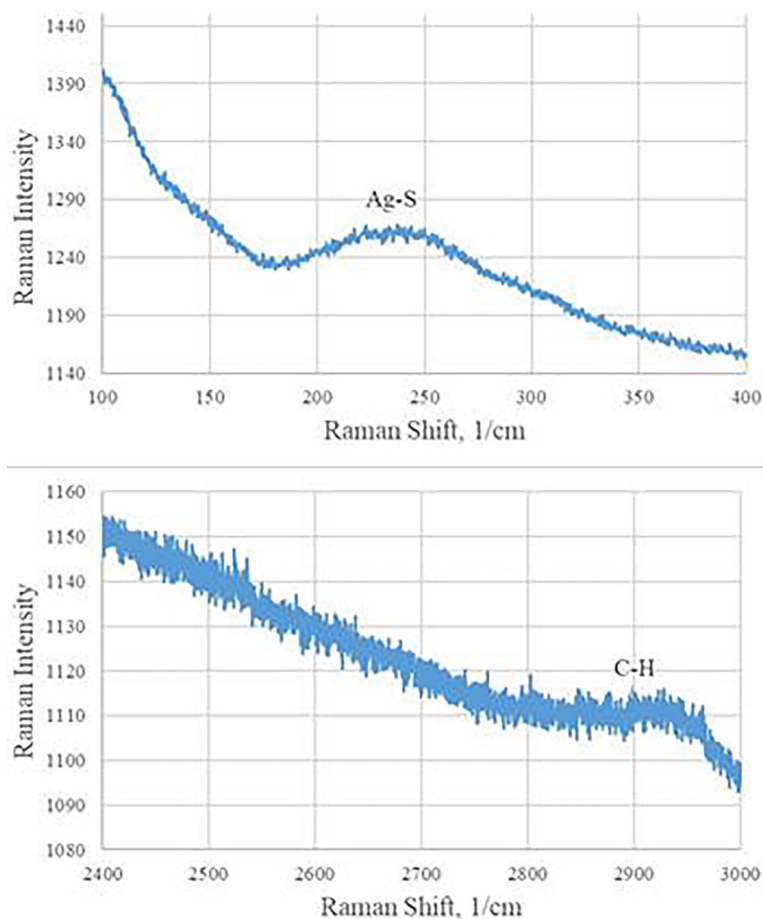


**Figure 7.** Raman spectrum of the sample (pH = 7.0, C(cys-H) =  $10^{-4}$  mol/L)

microstructures stabilized with an apple pectin solution. Figure 8 shows the size distribution of copper-silver bimetallic particles. The average particle size was  $(0.48 \pm 0.05) \times 10^3$  nm ( $p = 0.95$ ), thus these structures can be referred to as microparticles [Wan et al., 2020]. Studying the chemisorption of L-cysteine hydrochloride on the surface of bimetallic Cu-Ag microparticles and the structural formulas of the ionic forms of L-cysteine presented in Figure 9, one can be convinced that the concentration of L-cysteine hydrochloride is an important factor in assessing the chemisorption of the latter on the surface of dispersed phase particles.

According to the paper [Du et al., 2018], at its relatively high concentrations L-cysteine hydrochloride contributes to the aggregation of the dispersed phase and the entire loss of stability of the disperse system. This process especially proceeds in an acidic or alkaline media due to the interaction of the charged functional groups of L-cysteine and the electrical double layer of the dispersed phase. Therefore, the selection of optimal conditions for the successful chemisorption

of L-cysteine and maintaining the stability of the disperse system is an urgent task in the research. The pH values were adjusted in the range of 6–10.5, since aggregation and loss of stability of the dispersed system occur in a strongly alkaline medium, and hydrogen bonds with L-cysteine occur in a strongly acidic medium, which in turn also leads to aggregation [Du et al., 2018]. By means of two-factor ANOVA, the influence of factor A, factor B, and the interaction of these factors were confirmed (Table 1).

The values of the Fisher criterion, which are responsible for the influence of factor A, factor B, and the interaction of factors, exceed the critical values. The experimental values of the Fisher criterion in each case are more than the critical value, therefore, the concentration of L-cysteine hydrochloride and pH values affect the process of chemisorption of the corrosive agent simulator of the dispersed system. In addition, the interaction between these factors has been also proven.

Pearson correlation coefficient was found to determine if there was a correlation between the absorbance value at each concentration of

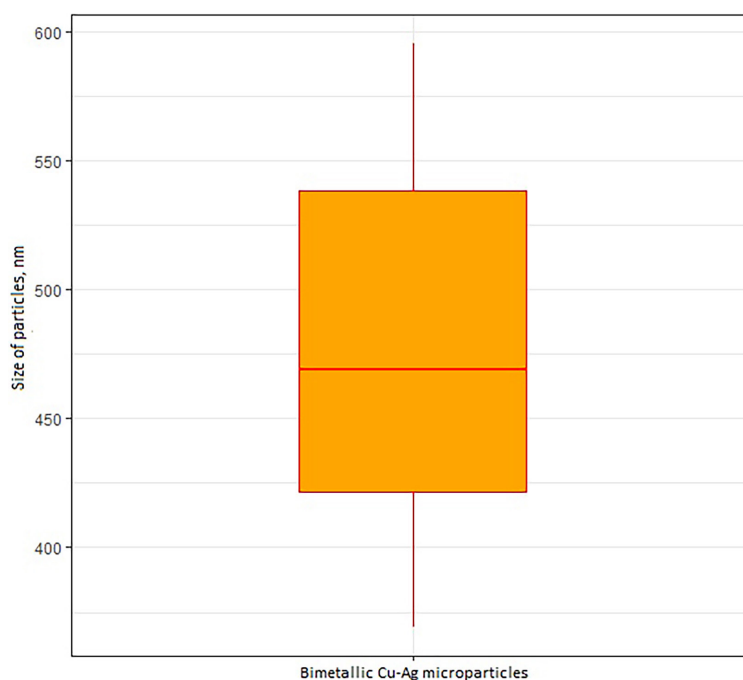


Figure 8. Box plot diagram of the sizes of bimetallic copper-silver microparticles

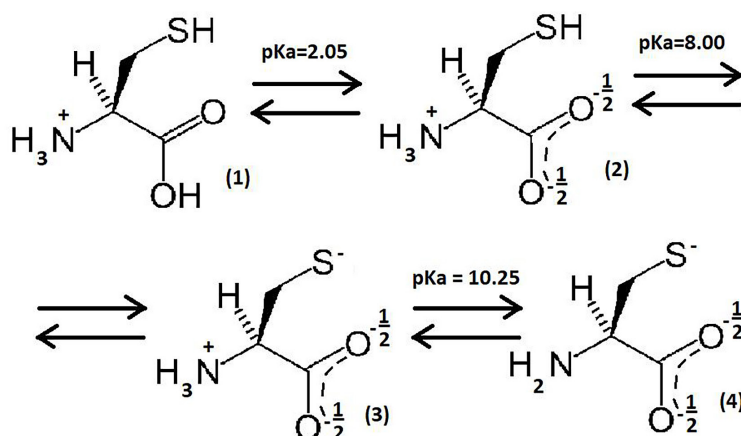


Figure 9. Formulas of ionic forms of L-cysteine [Wan et al., 2021]

Table 1. Values of the Fisher criterion depending on the source of variation

Factor	$F_{exp.}$	$F_{crit.}$
L-cysteine concentration	813.7	2.7
pH value	93.6	2.0
Interaction of factors	29.1	1.6

L-cysteine hydrochloride and the mole fraction of the neutral ionic form of L-cysteine hydrochloride (II form). In each case, it was more than 0.72, which indicates a high correlation between these parameters (Table 2). Therefore, the optimal ionic form for chemisorption of L-cysteine hydrochloride is

Table 2. Correlation analysis between the mole fraction of the second ionic form of L-cysteine and the absorbance at the  $i$ -th concentration of L-cysteine hydrochloride

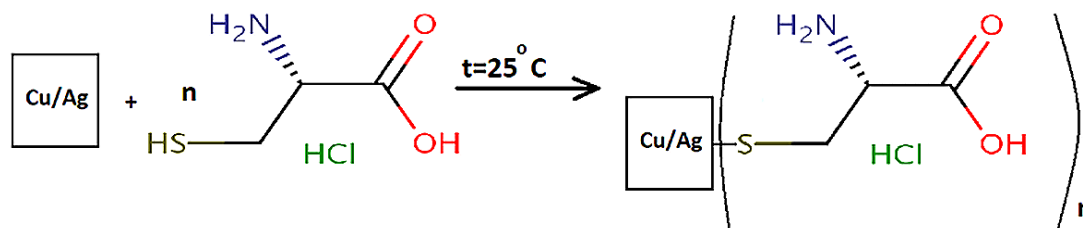
Concentration of L-cysteine hydrochloride, mol/L	Pearson correlation coefficient	Conclusion
$10^{-3}$	0.82	high correlation
$10^{-4}$	0.73	high correlation
$10^{-5}$	0.73	high correlation
$10^{-6}$	0.76	high correlation

the second ionic form (zwitter-ion) in accordance with Figure 9. To assess the minimum and adequate concentration of L-cysteine hydrochloride,



**Table 3.** Comparison of average light absorption values depending on the concentration of L-cysteine hydrochloride

No.	Comparison of concentrations (i и j)	$X_i$ , average absorbance at the i-th concentration	$X_j$ , average absorbance at j-th concentration	$ X_i - X_j $
1	$10^{-3}$ и $10^{-4}$	0.103	0.307	0.203
2	$10^{-3}$ и $10^{-5}$	0.103	0.315	0.211
3	$10^{-3}$ и $10^{-6}$	0.103	0.319	0.216
4	$10^{-4}$ и $10^{-5}$	0.307	0.315	0.008
5	$10^{-4}$ и $10^{-6}$	0.307	0.319	0.013
6	$10^{-5}$ и $10^{-6}$	0.315	0.319	0.005

**Figure 10.** Scheme of chemisorption of L-cysteine hydrochloride on the surface of bimetallic Cu-Ag microparticles**Table 3.** Comparison of average light absorption values depending on the concentration of L-cysteine hydrochloride

No.	Comparison of concentrations (i и j)	$X_i$ , average absorbance at the i-th concentration	$X_j$ , average absorbance at j-th concentration	$ X_i - X_j $
1	$10^{-3}$ и $10^{-4}$	0.103	0.307	0.203
2	$10^{-3}$ и $10^{-5}$	0.103	0.315	0.211
3	$10^{-3}$ и $10^{-6}$	0.103	0.319	0.216
4	$10^{-4}$ и $10^{-5}$	0.307	0.315	0.008
5	$10^{-4}$ и $10^{-6}$	0.307	0.319	0.013
6	$10^{-5}$ и $10^{-6}$	0.315	0.319	0.005

the Tukey-Kramer procedure for factor B was carried out in accordance with Table 3. The critical range of the Tukey-Kramer procedure for the concentration of L-cysteine hydrochloride was equal to 0.014. Therefore, the values of absorbance subtraction that are less than 0.014 indicate that differences between the respective adsorbate concentrations are negligible. Based on the results of Table 2, the differences between the concentrations of L-cysteine hydrochloride  $10^{-4}$ ,  $10^{-5}$ , and  $10^{-6}$  mol/L are not statistically significant ( $p = 0.95$ ). According to the information obtained from the analysis of the Raman spectrum of the sample, the chemisorption of L-cysteine hydrochloride proceeds through the formation of the Ag-S bond (Figure 10).

This phenomenon is explained by the fact that the affinity of silver for sulfur is greater than that of copper for sulfur [Wan et al., 2021]. The results of Raman spectroscopy and spectrophotometry in

studying the chemisorption of L-cysteine hydrochloride on the surface of bimetallic Cu-Ag microparticles are comparable in this case.

## CONCLUSION

Therefore, the possibility of chemical fixation of the corrosive modeling agent L-cysteine hydrochloride on the surface of dispersed phase have been verified. The results showed that this process proceeds according to the Ag-S bond formation mechanism. Thus, it is possible to transfer future experiments to real conditions with a layer of microparticles applied to the surface of the pipeline hull and reproduce near conditions for oil pipeline transportation. In this research, the conditions have been simulated with the temperature of 100 °C to remove most of the water,

when preparing samples for analysis with a Raman spectrometer, and the result turned out to be positive, i.e., chemisorption with the thiol group of cysteine occurred.

The practical result of this study is the further development of environmentally friendly methods for preventing corrosion of heating mains and pipelines under real operating conditions as well as the creation of practical approaches to choosing the most effective means of anti-corrosion protection depending on specific operating conditions.

### Acknowledgments

The authors express their gratitude to Ivan Igorevich Lyatun, staff scientist of International Research Center «Coherent X-Ray Optics for «Megascience» Units, Immanuel Kant Baltic Federal University (IKBFU) for carrying out SEM analysis of the bimetallic Cu-Ag microparticles samples.

### REFERENCES

1. Aleksandrova T., Aleksandrov A., Nikolaeva N. 2017. An investigation of the possibility of extraction of metals from heavy oil. *Mineral Processing and Extractive Metallurgy Review*, 38(2), 92–95.
2. Campos A., Troc N., Cottancin E., Pellarin M., Weissker H.C., Lermé J., Hillenkamp M. 2019. Plasmonic quantum size effects in silver nanoparticles are dominated by interfaces and local environments. *Nature Physics*, 15(3), 275–280.
3. Coutinho D.M., França D., Vanini G., Gomes A.O., Azevedo D.A. 2022. Understanding the molecular composition of petroleum and its distillation cuts. *Fuel*, 311, 122594.
4. Du J., Hu X., Zhang G., Wu X., Gong D. 2018. Colorimetric detection of cadmium in water using L-cysteine functionalized gold–silver nanoparticles. *Analytical Letters*, 51(18), 2906–2919.
5. Feng T., Meng X.F., Gao S.T., Feng C., Shang N.Z., Wang C. 2018. CuAg nanoparticles immobilized on biomass carbon nanospheres for high-efficiency hydrogen production from formaldehyde. *Catalysis Communications*, 113, 10–14.
6. Lewand L.R. 2002. The role of corrosive sulfur in transformers and transformer oil. In *Proceedings of the 69th Annual International Doble Client Conference*, Boston, MA, USA.
7. Mamyachenkov S.V., Adryshev A.K., Seraya N.V., Khairullina A.A., Daumova G.K. 2017. Nanostructured Complex Sorbent for Cleaning Heavy Metal Ions from Industrial Effluent. *Metallurgist*, 61(7–8), 615–623.
8. Peng J., Liang X. 2019. Progress in research on gold nanoparticles in cancer management. *Medicine*, 98(18).
9. Yu W.E., Gradov A.E., Ilyina E.A. 2020. Study of the influence of silver nanoparticles sol on the electrode EMF of the Jacobi-Daniel galvanic cell. *Modern innovative technologies of engineering training for mining and transport*, (1), 159–167.
10. Yu W.E., Shvets P.V., Gradov A.E. 2021. Study of chemisorption of l-cysteine hydrochloride on bimetallic cu-ag microparticles using physico-chemical methods of investigation. In *Current Issues and Innovations in Chemistry, Biology, Ecology, Agricultural Sciences and Science Education*, 120–124.
11. Wu W., Lei M., Yang S., Zhou L., Liu L., Xiao X., Roy V.A. 2015. A one-pot route to the synthesis of alloyed Cu/Ag bimetallic nanoparticles with different mass ratios for catalytic reduction of 4-nitrophenol. *Journal of Materials Chemistry A*, 3(7), 3450–3455.
12. Yang R., Zhang L., Li P., Yu L., Mao J., Wang X., Zhang, Q. 2018. A review of chemical composition and nutritional properties of minor vegetable oils in China. *Trends in food science & technology*, 74, 26–32.
13. Zhong Y., Liu M.M., Chen Y., Yang Y.J., Wu L.N., Bai F.Q., Liu A.L. 2020. A high-performance amperometric sensor based on a monodisperse Pt–Au bimetallic nanoporous electrode for determination of hydrogen peroxide released from living cells. *Microchimica Acta*, 187(9), 1–9.